

The Canadian Mineralogist
Vol. 45, pp. 631-648 (2007)
DOI: 10.2113/gscanmin.45.3.631

CHROMIAN SPINEL COMPOSITION AND THE PLATINUM-GROUP MINERALS OF THE PGE-RICH LOMA PEGUERA CHROMITITES, LOMA CARIBE PERIDOTITE, DOMINICAN REPUBLIC

JOAQUÍN A. PROENZA[§]

*Departament de Cristal·lografia, Mineralogia i Dipòsits Minerals. Facultat de Geologia.
Universitat de Barcelona, C/ Martí i Franquès s/n, E-08028 Barcelona, Spain*

FEDERICA ZACCARINI[¶]

*Department of Applied Geological Sciences and Geophysics,
The University of Leoben, P. Tunner Str, 5, A-8700 Leoben, Austria*

JOHN F. LEWIS

Department of Earth and Environmental Sciences, The George Washington University, Washington, D.C. 20052, U.S.A.

FRANCISCO LONGO

Falcondo XStrata Nickel, Box 1343, Santo Domingo, Dominican Republic

GIORGIO GARUTI

Department of Earth Sciences, The University of Modena and Reggio Emilia, S. Eufemia 19, I-41100 Modena, Italy

ABSTRACT

The Loma Peguera chromitites are located in the central part of Loma Caribe peridotite in the Cordillera Central of Dominican Republic. The chromitite bodies are hosted in typical mantle peridotites, have small size (less than a few meters across) and show massive textures. Primary chromite composition is Cr-rich ($0.74 < Cr\# < 0.78$) and exhibits systematically high Ti (average value: 0.84 wt% TiO₂) and Fe³⁺ (average value: 7.82 wt% Fe₂O₃). The total PGE concentrations vary from 1.82 to 2.04 ppm, and show an enrichment in Os + Ir + Ru relative to Rh + Pd + Pt. Among the latter group, a positive anomaly of Pt (249–269 ppb) is present as a result of the appearance of Pt-bearing alloys. The PGM assemblage comprises Ru, Os, Ir and Pt-rich phases, including laurite, irarsite, unknown Ru₃As₂, Ru–Os–Ir–Fe oxides, unknown Pt–Ir–Ni–Fe and Ru–Os–Ir–Pt–Fe–Ni alloys, native Ru and Ru-rich Ni–Fe alloy. The Loma Peguera chromitites are rather unusual in chemical composition compared with those commonly occurring in the Moho transition zone or from mantle harzburgites in ophiolites, but bear some similarity to chromitites from Uralian–Alaska-type complex. The Al₂O₃ and TiO₂ contents of the calculated composition of the melt in equilibrium with the Loma Peguera chromitites are similar to those from island-arc magmas and to some oceanic plateau basalts.

Keywords: platinum-group elements, platinum-group minerals, chromitites, Loma Peguera, Loma Caribe peridotite, Dominican Republic.

SOMMAIRE

Les chromitites de Loma Peguera sont situées dans la partie centrale du massif péridotitique de Loma Caribe, dans la Cordillère centrale de la République Dominicaine. On trouve ces amas de chromitite dans des péridotites typiques du manteau; ils sont de dimensions restreintes (moins de quelques mètres de diamètre) et possèdent une texture massive. La chromite primaire est riche en Cr ($0.74 < Cr\# < 0.78$), et enrichie en Ti (en moyenne, 0.84% de TiO₂ en poids) et en Fe³⁺ (en moyenne, 7.82% de

[§] E-mail address: japroenza@ub.edu

[¶] Present address: Instituto Andaluz de Ciencias de la Tierra, Universidad de Granada, E-18002 Granada, Spain.

Fe₂O₃). La concentration totale des éléments du groupe du platine varie de 1.82 à 2.04 ppm, et montre un enrichissement en Os + Ir + Ru par rapport à Rh + Pd + Pt. Parmi ce dernier groupe, nous notons une anomalie positive en Pt (249–269 ppb) à cause de la présence d'alliages porteurs de Pt. Les minéraux du groupe du platine sont surtout des minéraux riches en Ru, Os, Ir et Pt, y inclus laurite, irarsite, une phase de composition Ru₃As₂ méconnue, des oxydes de Ru–Os–Ir–Fe, des alliages méconnus de Pt–Ir–Ni–Fe et Ru–Os–Ir–Pt–Fe–Ni, le Ru natif et un alliage Ni–Fe riche en Ru. Les chromitites de Loma Peguera sont de composition chimique plutôt inhabituelle en comparaison des chromitites se trouvant dans la zone de transition au Moho, ou bien dans le manteau harzburgitique des ophiolites; elles ressemblent quelque peu aux chromitites provenant des complexes de type Ourale–Alaska. Les teneurs calculées en Al₂O₃ et TiO₂ du magma en équilibre avec les chromitites de Loma Peguera ressemblent à celles des magmas d'arcs insulaires, et à certains basaltes de plateaux océaniques.

(Traduit par la Rédaction)

Mots-clés: éléments du groupe du platine, minéraux du groupe du platine, chromitites, Loma Peguera, péridotite de Loma Caribe, République Dominicaine.

INTRODUCTION

Chromitites, in general, are considered as potential targets for platinum-group element (PGE) mineralization. The precious metals occur as microscopic, discrete inclusions of platinum-group minerals (PGM), in most cases enclosed in chromite crystals, and very occasionally within the silicate matrix of the chromitites. The minute grain-size and intricate textures of the PGM are the main reasons for the poor PGE recovery in many of the deposits. Presently, the PGE are recovered economically only from the UG2 chromitite layer of the Bushveld Complex in South Africa. This deposit has surpassed the famous Merensky Reef as the major source of platinum in the world (Cawthorn 1999). Apart from this economic interest, the mineralogy and genetic aspects of chromian spinel and associated PGM have presented challenges to students of mantle rocks and melting processes.

Recently, during mining activities for nickel, small bodies of chromitites have been found at Loma Peguera, in the central Dominican Republic, hosted in serpentinized peridotites of the Loma Caribe peridotite massif. Nickel-rich laterite is well developed over the serpentinized peridotites, and has been mined for nickel by Falconbridge Dominicana since 1970. In this paper, we report the first data on the composition of the chromian spinel, the concentration of PGE and a description of PGM in the Loma Peguera chromitites.

Reflected-light and scanning electron microscope investigations of polished sections, combined with quantitative analyses with an electron microprobe, have revealed a complex assemblage of PGM, comprising a few magmatic PGM and a large number of secondary PGM. The composition of the chromian spinel, together with the paragenesis and composition of PGM and their associated minerals, are used to discuss the genetic aspects of the mineralization.

GEOLOGICAL AND PETROLOGICAL BACKGROUND

Ophiolite-related ultramafic rocks crop out along the northern margin of the Caribbean Plate (Lewis *et*

al. 2006). One of these occurrences is the Loma Caribe peridotite, exposed in the Cordillera Central of the Dominican Republic (Fig. 1A). The peridotite body is about 4–5 km wide and extends for 95 km from La Vega to Loma Sierra Prieta north of Santo Domingo, but the southeastern part of the peridotite is exposed as thin fault slices only (Lewis & Jiménez 1991, Lewis *et al.* 2006). The peridotite further extends southeastward below the surface to the coast, as shown by aerial magnetic surveys and drilling. The Loma Caribe Peridotite was interpreted by Lewis & Jiménez (1991) to be serpentinized harzburgitic oceanic mantle forming part of a dismembered ophiolite complex.

The Loma Caribe peridotite forms the core of the Median Belt of Mesozoic age, in the central Dominican Republic (Bowin 1966, Lewis & Draper 1990); that belt includes two major metamorphosed units: 1) the Lower Cretaceous, dominantly volcanic Maimon Formation, with a bimodal suite composed of primitive island-arc tholeiite and rhyolite, to the north of the peridotite belt (Lewis *et al.* 2000, 2002); 2) the Upper Jurassic to Lower Cretaceous Duarte Complex, composed of enriched mid-ocean-ridge basalts (E-MORB), which have compositions comparable with oceanic plateau basalt, related to a mantle plume, which lies to the south (Lewis *et al.* 2002). The Maimon Formation is separated from the Loma Caribe peridotite massif by a narrow belt of mainly unfoliated basaltic rocks of the Peralvillo Formation, of apparent Late Cretaceous age. To the south, the Siete Cabezas Formation, of Cenomanian age, consisting of basalt flows with intercalated cherts and volcanoclastic units, separates the Duarte complex from the Loma Caribe peridotite (Lewis & Draper 1990, Lewis *et al.* 2002). The Río Verde Complex lies within and along the strike of the Loma Caribe peridotite body and consists of metabasic rocks, gabbros, diabases and basalts (Fig. 1; Draper *et al.* 1996, Lewis *et al.* 2002). Because of faulting, the tectonostratigraphic relationships between the basaltic and ultramafic lithologies are unknown. The Loma Caribe ultramafic rocks are considered to have been emplaced first, as early as the late Albian, as a result of the collision of an oceanic plateau (the Duarte plateau terrane) with the primi-

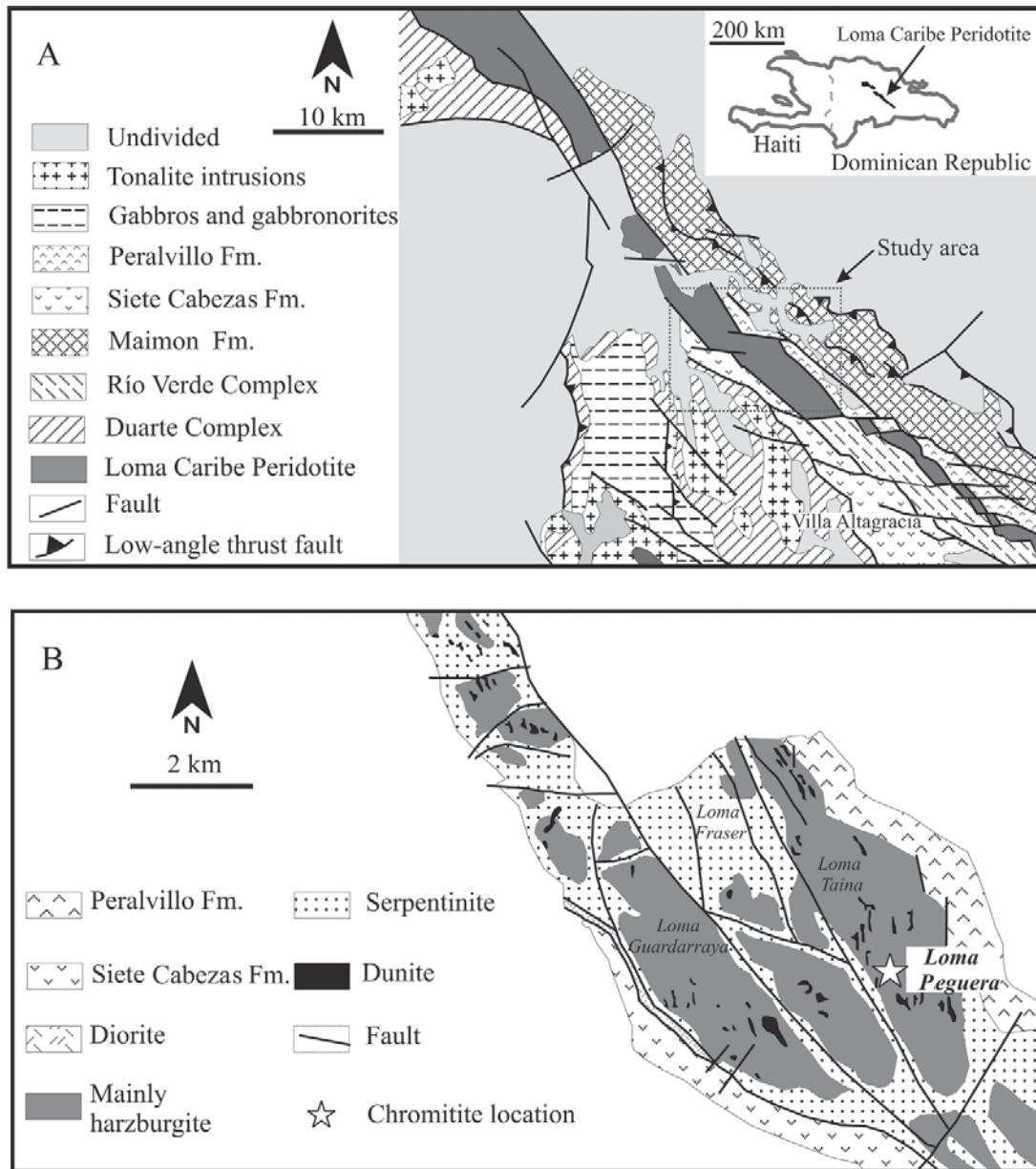


FIG. 1. Geographical location and simplified geological map of the central section of the Loma Caribe peridotite, modified from Bowin (1966) and Escuder-Viruete *et al.* (2002). B) Geological sketch-map of south-central part of the Loma Caribe peridotite showing the location of the Loma Peguera area, modified from Haldemann *et al.* (1979).

tive Caribbean island arc (Maimon–Amina terrane) in Aptian time (Draper *et al.* 1996, Lewis *et al.* 2002).

The Loma Caribe peridotite is bounded by major faults; no stratigraphic boundaries with other units have been observed. Major faults (shear zones) within the

body strike parallel to the northwest trend of the massif and to the foliation (Haldemann *et al.* 1979; Fig. 1B). Most of the ultramafic bodies consist of harzburgite, with clinopyroxene-rich harzburgite and small amounts of lherzolite. These ultramafic rocks, which are about

20–30% serpentinized, make up about 50–60% of the outcrop; the remainder consists mainly of serpentinite with talc (Fig. 1B). Small masses of dunite within harzburgite have been mapped and are particularly concentrated in the Loma Peguera area, where the main concentration of the chromitites has been found (Fig. 1B). These bodies of dunite were considered to be dikes by Haldemann *et al.* (1979). Although it is difficult to determine their shape in detail, the masses of dunite are small and discontinuous. Most are lensoid or tabular. The larger bodies are 500 m in length, but many measure no more than 10 m across. Their contacts with harzburgite are mainly irregular. Thus they are probably the same as the small irregular “patches” of dunite reported from the mantle section in many ophiolites (Nicolas 1989). Most of the dunite bodies are highly serpentinized, but reasonably fresh dunite with only minor serpentine can be found.

The peridotites typically show porphyroclastic and coarse-grained granoblastic textures, with orthopyroxene crystals strongly deformed (Lewis & Jiménez 1991, Lewis *et al.* 2005, 2006). The Cr/(Cr + Al) value of accessory chromian spinel varies from 0.30 in lherzolite to 0.88 in dunite. These large compositional variations indicate the occurrence of peridotites with very different histories of melting (Lewis *et al.* 2005). Harzburgite and dunite have homogeneous HREE contents and are characterized by relatively flat LREE and a steep HREE fractionated segment. These patterns are similar to those of depleted peridotite from ophiolite in eastern Cuba (Proenza *et al.* 1999, Marchesi *et al.* 2006), and to those of peridotite from the Izu–Bonin–Mariana forearc (Parkinson & Pearce 1998). They have been interpreted to result from partial melting and mantle interaction with ascending melts at a suprasubduction zone (Lewis *et al.* 2005). In contrast, the lherzolites from Loma Caribe peridotite are enriched in MREE and HREE compared to the harzburgite and dunite. The REE patterns have low LREE/MREE and MREE/HREE values consistent with partial melting in the garnet peridotite facies (Lewis *et al.* 2005). According to these authors, the upper mantle rocks present in Loma Caribe peridotite probably include rocks from the suboceanic mantle, including mantle underneath the oceanic ridge, oceanic plateau and island arc.

SAMPLE LOCATION AND ANALYTICAL TECHNIQUES

The chromitite samples analyzed are from the area now largely mined out south of the Falcondo plant at Loma Peguera (Fig. 1B), and were collected from four outcrops. Petrographic studies as well as analyses of chromian spinel, silicate and PGM were performed on 10 polished thin sections and 22 polished sections.

The analyses of the chromian spinel and silicate were done with a four-channel CAMECA SX50 electron microprobe at the Serveis Científicotècnics of the

Universitat de Barcelona. Mineral compositions were obtained by analyzing several grains in each section. The analytical conditions were: accelerating voltage 20 kV, beam current 20 nA, beam diameter 2 μm , and a counting time of 10 seconds per element. Calibrations were performed using natural and synthetic reference materials: chromite (Cr, Al, Fe), periclase (Mg), rhodinite (Mn), rutile (Ti), NiO (Ni) and metallic V. The proportion of Fe³⁺ in chromian spinel was calculated assuming stoichiometry. Selected analytical results for chromian spinel from the chromitites are listed in Table 1, and for accessory chromian spinel from associated peridotite samples in Table 2.

Two samples of chromitite were analyzed for platinum-group elements (PGE) and Au in the Genalysis Laboratory Services Pty. Ltd. at Maddington, Western Australia. The samples were analyzed by inductively coupled plasma – mass spectrometry (ICP–MS) after concentration with nickel sulfide fire-assay collection. Detection limits were 1 ppb for Rh, and 2 ppb for Os, Ir, Ru, Pt, Pd, and 5 ppb for Au. Gold is below detection limits in all the analyzed samples. Analytical results are listed in Table 3.

The PGM were first located on 22 polished sections (about 3 cm² each) using an optical microscope. They were then investigated by electron microscopy and by electron-microprobe analysis. The SEM images were obtained with a Philips XL–40 scanning electron

TABLE 1. REPRESENTATIVE RESULTS OF ELECTRON-MICROPROBE ANALYSES OF CHROMITE FROM THE LOMA PEGUERA CHROMITITE

	95-91	96-92	0326i	0325f	98c1	98c2	98c3	98c4	98c6	98c7
SiO ₂ , wt%	0.14	0.10	0.16	0.16	0.15	0.18	0.13	0.13	0.15	0.15
TiO ₂	0.88	0.79	0.84	0.84	0.91	0.77	0.63	0.92	0.91	1.15
Al ₂ O ₃	9.96	10.24	10.23	10.35	10.47	10.32	11.97	9.97	10.23	10.83
Cr ₂ O ₃	52.89	51.16	51.42	51.12	50.77	50.94	51.67	51.72	51.67	50.89
Fe ₂ O ₃	6.35	8.22	7.63	8.25	8.07	8.28	6.51	7.75	7.54	7.27
FeO	19.94	19.57	19.88	19.49	19.29	19.46	19.33	20.11	20.17	20.33
V ₂ O ₅	0.12	0.10	0.16	0.12	0.12	0.17	0.19	0.17	0.12	0.14
MnO	0.32	0.36	0.33	0.35	0.35	0.37	0.30	0.35	0.33	0.39
MgO	9.09	9.18	9.08	9.31	9.48	9.28	9.71	9.03	9.01	9.18
ZnO	0.21	0.18	0.17	0.20	0.11	0.15	0.22	0.13	0.24	0.15
NiO	0.21	0.37	0.39	0.51	0.43	0.50	0.20	0.33	0.33	0.25
Total	100.11	100.27	100.29	100.70	100.15	100.42	100.86	100.63	100.70	100.73
Si <i>apfu</i>	0.04	0.02	0.04	0.04	0.04	0.05	0.03	0.03	0.04	0.04
Ti	0.18	0.16	0.17	0.17	0.18	0.15	0.13	0.18	0.18	0.23
Al	3.13	3.21	3.21	3.22	3.27	3.22	3.69	3.12	3.19	3.37
Cr	11.14	10.75	10.82	10.69	10.65	10.68	10.68	10.86	10.83	10.62
Fe ³⁺	1.27	1.65	1.53	1.64	1.61	1.66	1.28	1.55	1.50	1.45
Fe ²⁺	4.44	4.35	4.42	4.31	4.28	4.32	4.22	4.46	4.47	4.49
V	0.02	0.02	0.03	0.02	0.02	0.03	0.04	0.04	0.02	0.03
Mn	0.07	0.08	0.07	0.08	0.08	0.08	0.06	0.08	0.07	0.09
Mg	3.61	3.64	3.60	3.67	3.75	3.66	3.78	3.58	3.56	3.61
Zn	0.04	0.03	0.03	0.04	0.02	0.03	0.04	0.02	0.05	0.03
Ni	0.05	0.08	0.08	0.11	0.09	0.10	0.04	0.07	0.07	0.06
Cr#	0.78	0.77	0.77	0.77	0.77	0.77	0.74	0.78	0.77	0.76
Mg#	0.45	0.46	0.45	0.46	0.47	0.46	0.47	0.45	0.44	0.45
Fe ³⁺ #	0.08	0.11	0.10	0.11	0.10	0.11	0.08	0.10	0.10	0.09

Cations calculated on the basis of 32 atoms of oxygen.

microscope at the Inter-department Instrumental Center (CIGS) of the University of Modena and Reggio Emilia, with an accelerating voltage of 20–30 kV and a beam current of 2–10 nA. Quantitative analyses of the PGM were performed at the Department of Earth Sciences, University of Modena and Reggio Emilia, using an ARL-SEM-Q electron microprobe operated in WDS mode at an accelerating voltage of 15–25 kV and a beam current of 15–20 nA, with a beam diameter of about 1 μm . On-line ZAF data-reduction and automatic correction for the interferences $\text{FeK}\beta\text{-CoK}\alpha$, Ru-Rh , Ir-Cu , and Rh-Pd were performed using the PROBE software package (version 1996) by J. Donovan. The X-ray $\text{K}\alpha$ lines were used for S, Cr, Fe, Ni, and Cu, $\text{L}\alpha$ lines for Ir, Ru, Rh, Pt, Pd, and As, and $\text{M}\alpha$ line for Os. Pure metals were used as standards for the PGE, natural chromite for Cr and synthetic NiAs, FeS_2 and CuFeS_2 for Ni, Fe, Cu, S, and As. The interferences Ru-Rh , Ir-Cu , and Ru-Pd were automatically corrected on-line. Representative results of the analyses of the PGM, base-metal sulfides and alloys are listed in Table 4.

THE LOMA PEGUERA CHROMITITES

Mode of occurrence and petrography

The chromitite bodies at Loma Peguera occur as discontinuous lenses or pods surrounded by variably

TABLE 2. REPRESENTATIVE RESULTS OF ELECTRON-MICROPROBE ANALYSES OF ACCESSORY CHROMIAN SPINEL FROM THE LOMA PEGUERA PERIDOTITES

	M4a	M4b	M4c	TL 113a	TL 113b	TL 113c	94- 48a	94- 48b	94- 48c
TiO_2 wt%	0.06	0.06	0.05	0.02	0.08	0.06	0.05	0.06	0.07
Al_2O_3	5.76	5.80	5.20	17.88	16.40	16.38	34.75	40.20	38.61
V_2O_5	0.21	0.19	0.18	0.26	0.33	0.27	0.17	0.13	0.17
Cr_2O_3	55.48	55.38	55.88	48.76	51.08	50.96	33.53	26.01	27.72
Fe_2O_3	8.17	8.64	8.97	2.64	2.23	2.43	1.79	2.61	2.80
FeO	23.08	22.83	22.62	18.23	18.74	18.89	14.69	15.12	15.77
MgO	5.93	6.14	6.25	10.27	9.96	9.92	14.77	14.90	14.44
MnO	0.41	0.48	0.44	0.34	0.36	0.27	0.21	0.22	0.19
ZnO	0.24	0.23	0.21	0.28	0.25	0.35	0.20	0.34	0.27
NiO	0.00	0.01	0.00	0.01	0.05	0.01	0.03	0.01	0.00
Total	99.35	99.75	99.81	98.69	99.48	99.54	100.18	99.58	100.04
Ti <i>appfu</i>	0.01	0.01	0.01	0.00	0.02	0.01	0.01	0.01	0.01
Al	1.90	1.91	1.71	5.45	5.00	5.00	9.49	10.80	10.43
V	0.05	0.04	0.04	0.05	0.07	0.06	0.03	0.02	0.03
Cr	12.29	12.20	12.33	9.96	10.45	10.43	6.14	4.69	5.02
Fe^{3+}	1.72	1.81	1.89	0.51	0.43	0.47	0.31	0.45	0.48
Fe^{2+}	5.41	5.32	5.28	3.94	4.06	4.09	2.85	2.88	3.02
Mg	2.48	2.55	2.60	3.96	3.84	3.83	5.10	5.06	4.93
Mn	0.10	0.11	0.10	0.07	0.08	0.06	0.04	0.04	0.04
Zn	0.05	0.05	0.05	0.07	0.05	0.06	0.04	0.05	0.05
Ni	0.00	0.00	0.00	0.00	0.01	0.00	0.01	0.00	0.00
Cr#	0.87	0.86	0.88	0.65	0.68	0.68	0.39	0.30	0.33
Mg#	0.31	0.32	0.33	0.50	0.49	0.48	0.64	0.64	0.62
Fe^{3+} #	0.11	0.11	0.12	0.03	0.03	0.03	0.02	0.03	0.03

M4a, b, c: dunite, TL-113a, b, c: harzburgite, 94-48a, b, c: lherzolite. Cations calculated on the basis of 32 atoms of oxygen.

thick serpentinites mainly derived from dunite. The largest body found, now removed by the mining operations, measured 6 m across, but most have a small size, measuring <1 m in thickness and <10 m in length (Figs. 2A, B, C, D). Some of the chromitite bodies studied seem to be stretched out parallel to the mantle tectonite fabric in the enclosing peridotites, and this has resulted in boudinage structures (Fig. 2C). In one area, a series of parallel and cross-cutting faults have segmented and displaced the lenses of chromitite (Fig. 2D). Irrespective of limited outcrops, all chromitite bodies at Loma Peguera occur within a peridotite tectonite, and have a lens-like shape with limited lateral extent. In this respect, according to the classification of Thayer (1964), the Loma Peguera chromitite shows a similarity to podiform (ophiolitic) chromite deposits.

All samples of chromitite show typically massive textures (>95 vol.% chromian spinel), and are composed of large (3–7 mm in diameter) anhedral crystals of chromian spinel (Fig. 2E). In general, intense fracturing is observed in practically all chromitite samples. However, chromian spinel crystals are homogeneous in thin section (Fig. 2F), and chemical zoning is limited to the development of a thin rim of ferrian chromite, along grain boundaries and cracks.

No primary silicate minerals are preserved in the matrix of any of the chromitite samples studied. Interstitial minerals are mainly chlorite (clinocllore with up to 3.1 wt% of Cr_2O_3) and minor serpentine, accompanied by pentlandite, and Fe–Ni alloy as accessories. Chlorite and serpentine also occur as inclusions in the grains of chromian spinel.

Composition of the chromian spinel

The chromitite samples analyzed in this work preserve unaltered chromite in the cores of grains. Their SiO_2 contents are invariably low (<0.2 wt%) and unrelated to the contents of the other major oxides. Only those compositions obtained in these unaltered cores have been considered in the interpretation of the primary chromian spinel, and used for petrogenetic indications. For convenience, the chromian spinel in the chromitite and dunite will be referred to as chromite,

TABLE 3. CONCENTRATIONS (ppb) OF NOBLE METALS IN THE LOMA PEGUERA CHROMITITES

Sample	Os	Ir	Ru	Rh	Pt	Pd	Au
95-91	352	430	695	87	249	7	<5
95-92	432	461	778	90	269	6	<5
Anomalies*							
95-91		1.08	1.12	0.66	7.77		
95-92		1.01	1.15	0.63	8.35		

* Calculated according to the method of Garuti *et al.* (1997a).

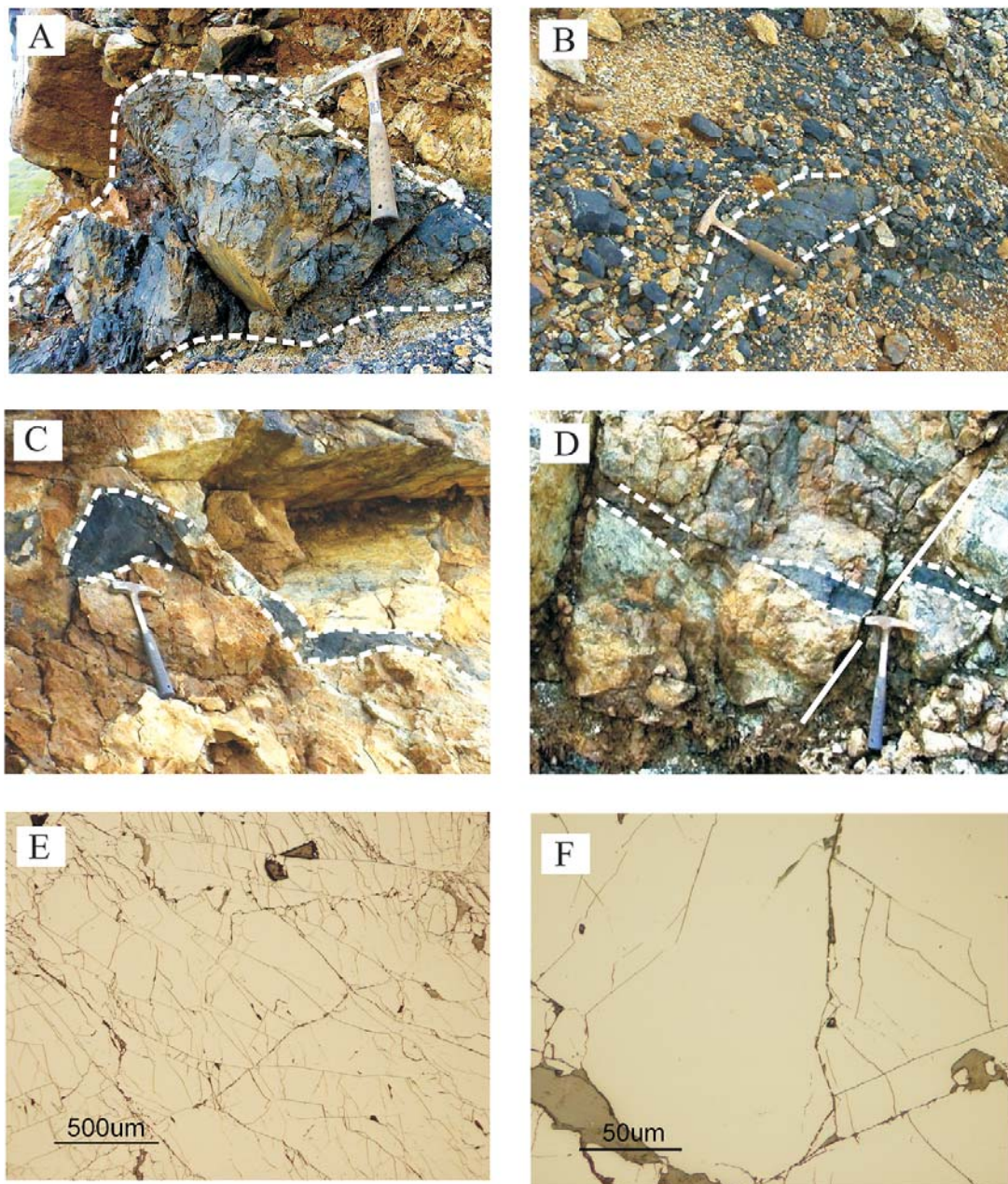


FIG. 2. A–D. Photographs of lenticular bodies of massive chromitite within serpentinite of dunite origin from Loma Peguera area, Dominican Republic. E) Highly fractured elongate grains in massive chromitite (reflected-light photomicrographs). F) Detail of an unzoned grain of chromite; note that extensive oxidation to ferrian chromite along cracks and grain boundaries has not taken place (reflected-light photomicrograph).

that in harzburgite will be referred to as magnesiochromite, and that in lherzolite will be referred to as spinel (Fig. 3A).

The composition of primary chromite from the Loma Peguera chromitite is remarkably homogeneous in terms of Cr# [$\text{Cr}/(\text{Cr} + \text{Al})$] and Mg# [$\text{Mg}/(\text{Mg} + \text{Fe}^{2+})$] (Fig. 3A). The Cr# varies from 0.74 to 0.78, corresponding to Cr_2O_3 contents between 49.42 and 53.72 wt%, and Al_2O_3 between 9.30 and 11.38 wt%. The Mg# is relatively low, from 0.44 to 0.50. The Loma Peguera chromite exhibits systematically high TiO_2 (0.52–1.15 wt%) and Fe_2O_3 (5.31–8.50 wt%) contents. The $\text{Fe}^{3+}\#$ [$\text{Fe}^{3+}/(\text{Fe}^{3+} + \text{Cr} + \text{Al})$] ranges between 0.09 and 0.11. Minor amounts of MnO (0.28–0.46 wt%), V_2O_5 (<0.20 wt%), ZnO (<0.27 wt%) also were detected (Table 1). NiO contents are relatively high (up to 0.5 wt%, and on average, 0.3 wt%) compared to those in typical podiform chromitites where data are available (<0.3 wt%, *e.g.*, Lorand & Ceuleneer 1989).

On a Cr# versus Mg# diagram (Fig. 3A), chromite samples from the Loma Peguera chromitites overlap with the fields of chromite from stratiform complexes and Cr-rich ophiolitic chromite. However, the Loma Peguera chromite is slightly higher in Cr# and is lower in Mg# compared with Cr-rich chromitites from the

eastern Cuba ophiolite (Fig. 3A, Proenza *et al.* 1999). In the Cr# versus TiO_2 plot (Fig. 3B), the chromite compositions at Loma Peguera plot outside the fields defined by eastern Cuba podiform chromitites (Proenza *et al.* 1999), as well as by chromian spinel in boninites and mid-oceanic-ridge basalts (MORB) (Arai 1992).

Compositions of Loma Peguera chromite samples differ from high-Cr, low-Ti podiform chromitites hosted in the mantle section of ophiolitic complexes. The compilation of spinel from ophiolitic chromitites by Barnes & Roeder (2001, their Figs. 5 and 6) shows no data points comparable with those of the Loma Peguera chromitites. To the best of our knowledge, chromite compositions comparable with those of the Loma Peguera chromitites have not been previously reported from podiform chromitites found in the Moho Transition Zone (MTZ) and mantle tectonites of ophiolitic complexes.

On the other hand, the accessory chromian spinel from associated peridotites is compositionally distinct from that of chromitites (Figs. 3A, B). Chromian spinel from dunites at Loma Peguera has a higher Cr# (0.86–0.88) compared with that of the chromitites, but shows a lower Mg# (0.31–0.39) and TiO_2 contents (<0.13 wt%). Chromian spinel from the associated

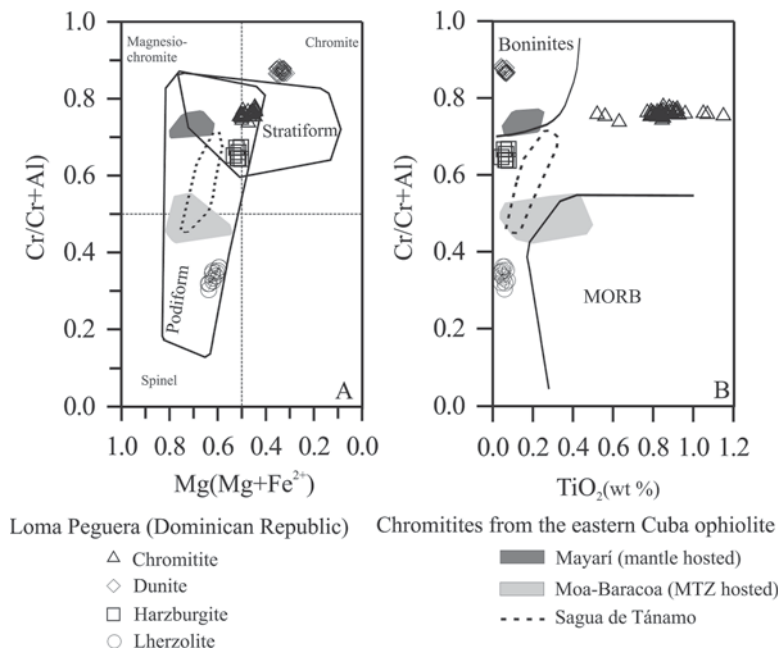


FIG. 3. A) #Cr [$\text{Cr}/(\text{Cr} + \text{Al})$] versus #Mg [$\text{Mg}/(\text{Mg} + \text{Fe})$], and B) #Cr versus TiO_2 content for chromian spinel in the Loma Peguera chromitites and their associated peridotites. The fields labeled “podiform” and “stratiform” are after Irvine (1967) and Leblanc & Nicolas (1992), respectively. Boninitic and MORB fields were defined by Arai (1992). The fields defined by chromitites from the eastern Cuba ophiolite, after Proenza *et al.* (1999), are shown for comparison.

harzburgites has a lower Cr# (0.65–0.69), TiO₂ contents (<0.1 wt%) and similar Mg# (0.48–0.50) than that found in the chromitites. Chromian spinel in the Iherzolites shows a lower Cr# (0.32–0.41), TiO₂ contents (<0.1 wt%) and higher Mg# (0.58–0.80), and thus corresponds to magnesiochromite.

LEVELS OF PGE CONCENTRATION

The Loma Peguera chromitites are characterized by high concentrations of the PGE, with the total PGE content for each of the two samples ranging between 1.82 to 2.04 ppm (Table 3). Also listed in Table 3 are the anomaly values for Ir, Ru, Rh and Pt calculated from the formula given by Garuti *et al.* (1997a) using the C1 chondrite values instead of the primitive mantle. Chondrite-normalized patterns of distribution are presented in Figure 4, and compared with those obtained for chromitites hosted in the ophiolitic mantle. The general trend resembles that of mantle-hosted ophiolitic chromitites, being characterized by an enrichment in the

Os + Ir + Ru (IPGE) relative to Rh + Pd + Pt (PPGE), which causes a negative slope between IPGE and PPGE. However, the Loma Peguera chromitites display a general enrichment in all the PGE, except for Pd, with Os, Ir, Ru poorly fractionated, forming a relatively flat pattern. Only Ru shows a very weak positive anomaly (1.12–1.15). Among the PPGE, a positive anomaly of Pt (7.77–8.35) is present, whereas Rh displays a negative anomaly (0.63–0.66).

MINERALOGY OF THE PGE

Platinum-group minerals were found in 14 polished sections of chromitite, with an average frequency of about two grains per square centimeter. Generally, they are less than 10 µm in size and consist of Ru, Os, Ir and Pt phases. On the basis of textural position, paragenesis and composition, the PGM can be divided into two categories. 1) The primary PGM, formed at the high-temperature magmatic stage before and during the crystallization of chromite, consist only of laurite, irarsite, and an unknown PGM corresponding to the formula Ru₃As₂ (Fig. 5, Table 4). 2) The secondary PGM, probably formed at a relatively low temperature during some postmagmatic event, consist of Ru–Os–Ir–Fe oxides, unknown Pt–Ir–Fe–Ni and Ru–Os–Ir–Pt–Fe–Ni alloys, native Ru and Ru-rich Ni–Fe alloy (Figs. 6, 7, Table 4).

The assemblages and composition of primary PGM

Only three grains, two of laurite and an unknown Ru arsenide (Ru₃As₂), are tentatively classified as magmatic PGM in the Loma Peguera chromitites (Fig. 5). They occur enclosed in fresh chromite and, although they are in contact with chlorite and Ru–Os–Ir–Fe oxide, their shape and composition suggest a primary origin. Laurite forms a single-phase grain (Fig. 5A), or it occurs associated with irarsite (Fig. 5B). The composition of the primary laurite (Fig. 8, Table 4), in terms of Ru–Os–Ir, is similar to that of most of the magmatic laurite (Garuti *et al.* 1999a, b, Zaccarini *et al.* 2004, 2005, Gervilla *et al.* 2005), containing Os and Ir in solid solution, up to 16.44 wt% and 13.09 wt%, respectively. However, the composition of the Loma Peguera laurite is not consistent with the alteration trend proposed for the secondary laurite associated with the Tehuiztingo chromitites in Mexico (Zaccarini *et al.* 2005). These authors showed that the altered laurite is typically depleted in Os, and tends to plot toward the composition of the pure Ru-end member. One polygonal grain (about 5 µm in size), corresponding to the formula Ru₃As₂ (Fig. 5C, Table 4), has been found in contact with chlorite and a Ru–Os–Ir–Fe oxide. The Ru arsenide is white in color, possibly cubic, and displays a sharp extinction. To the best of our knowledge, this mineral potentially represents a new mineral species, but the grain is too small to characterize.

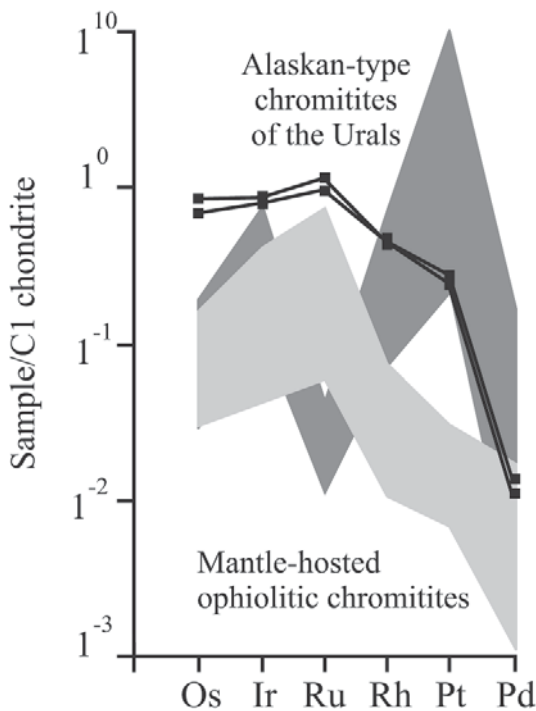


FIG. 4. Chondrite-normalized (Naldrett & Duke 1980) patterns of the Loma Peguera chromitites and comparison with the chromitites hosted in the ophiolitic mantle. Data from Economou Eliopoulos (1996), Gauthier *et al.* (1990), Kojonen *et al.* (2003), McElduff & Stumpfl (1990), Proenza *et al.* (1999, 2004) and Zhou *et al.* (1998). Data for Alaskan-type complexes of the Urals are from Garuti *et al.* (2003, 2005).

The assemblages and composition of secondary PGM

Most of the PGM discovered in Loma Peguera chromitites are secondary, and they occur in the chromite along fissures and cracks, along which ferric chromite and chlorite are developed (Fig. 6). More rarely, they are

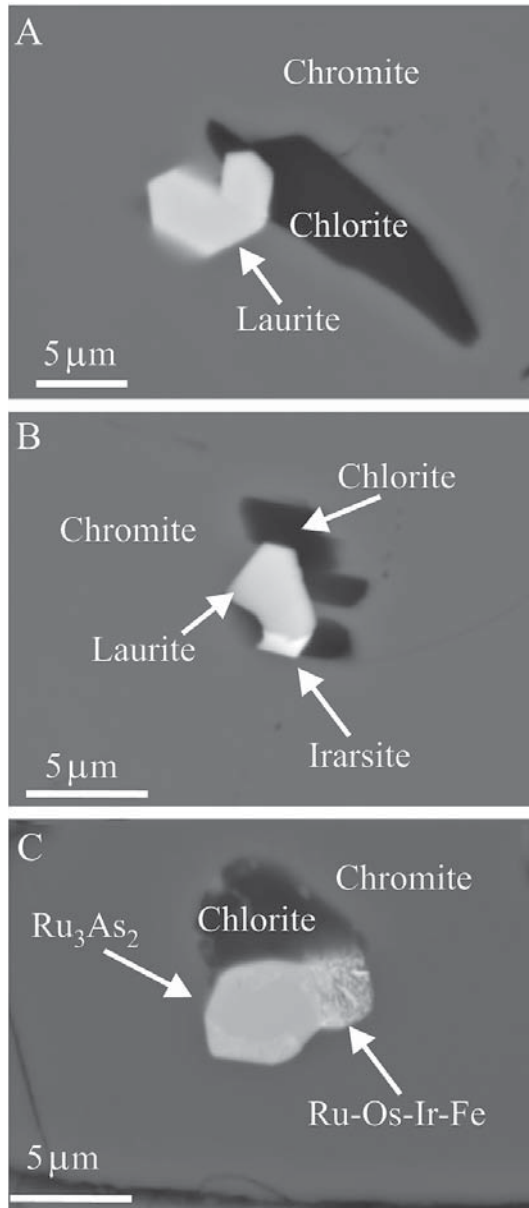


FIG. 5. BSE images showing morphology, texture and mineral assemblages of magmatic PGM in the Loma Peguera chromitites.

found in the chlorite-dominant matrix of the chromite. The secondary PGM are characterized by an irregular shape, rugged surface and high porosity (Fig. 6). In some cases, the PGM grains consist of two phases intimately intergrown, one containing an oxide and the other composed of a sulfide or a PGE alloy (Figs. 6A, C). The Ru–Os–Ir–Fe oxides are the most abundant PGM in the Loma Peguera chromitites. They display optical properties and compositions similar to the PGM oxides reported in the Vourinos and Nurali chromitites, located in Greece and Urals, respectively (Garuti & Zaccarini 1997, Garuti *et al.* 1997b). Electron-microprobe data (at.%) plotted in Figure 8 reveal that the compositions of the Ru–Os–Ir–Fe oxides are very similar to those of sulfides of the laurite–erlichmanite series. As a consequence, their chemical compositions in terms of Ru–Os–Ir proportions strongly suggest an origin of these oxides by a progressive desulfuration and further oxidation of primary laurite, as shown in Figure 8. The texture of these grains indicates that the oxide represents a late replacement of the former phases, mainly laurite (Fig. 6C). The desulfuration process is also supported by the finding of numerous grains of pentlandite rimmed by awaruite, associated with serpentine (Fig. 7A). A grain of awaruite, found in contact with serpentine and ferric chromite, contains small spots of native Ru (Fig. 7B). Several secondary alloys containing base metals (BM) and PGE in various proportions have also been analyzed. These alloys are characterized by a wide range of composition and cannot be unambiguously ascribed to any known phase. Their compositions, plotted as atomic % in the Os + Ir + Ru – Pt + (Rh + Pd) – Fe + Ni diagram (Fig. 9), show that in most cases, these alloys are not PGM *sensu stricto*, but should more correctly be classified as PGE-bearing BM alloys (Fig. 9). They contain substantial amounts of Pt (5.8–24.16 at.%), and can be tentatively classified on the basis of composition as: 1) Pt–Ir–Fe–Ni alloy ($\text{Pt}_{14-24}\text{Ir}_{2-15}\text{Fe}_{30-45}\text{Ni}_{23-41}$, $n = 6$ anal.) containing minor amounts of Rh and Cu, 2) Ru–Os–Ir–Pt–Fe–Ni alloy ($\text{Ru}_{15-22}\text{Os}_{10-14}\text{Ir}_{14-18}\text{Pt}_{2-6}\text{Fe}_{29-32}\text{Ni}_{13-18}$, $n = 3$) with minor Rh and Cu, and 3) Ru–Os–Ir–Rh–Fe–Ni alloy ($\text{Ru}_{16}\text{Os}_{12}\text{Ir}_{44}\text{Rh}_4\text{Fe}_{20}\text{Ni}_{13}$, $n = 1$) (Table 4).

DISCUSSION

Chromite composition and origin of the Loma Peguera chromitites

The chromite composition of the Loma Peguera chromitites is characterized by relatively high content of Cr_2O_3 , Fe_2O_3 , and TiO_2 . This chemical composition is clearly different from typical podiform (ophiolitic) chromite recorded in the literature (Figs. 10A, B). Chromite in small podiform deposits with high Cr# (0.62–0.85) and ferric iron contents (up to 8.95 wt% of Fe_2O_3) have been described in ultrabasic rocks from the Bragança massif (Portugal), and were interpreted as

TABLE 4. SELECTED RESULTS OF ELECTRON-MICROPROBE ANALYSES OF PGM AND BASE-METAL MINERALS FROM THE LOMA PEGUERA CHROMITITE

	Os	Ir	Ru	Rh	Pt	Pd	Fe	Ni	Cu	S	As	O*	Total
Laurite													
98c6 2 2 wt%	15.93	4.82	38.80	1.41	0.00	0.00	1.34	0.14	0.05	35.39	0.00		97.88
98c6 2 3	16.44	3.53	37.48	1.27	0.00	0.44	1.45	0.33	0.00	35.68	0.00		96.62
98c6 3 2	15.30	13.09	30.90	0.87	0.00	0.00	4.04	0.20	0.00	30.91	3.47		98.78
Unknown Ru₃As₂													
0325f 1 1	22.6	2.21	35.31	0.85			3.23	0.08			30.17		94.45
Partially desulfurized laurite													
98c6 4 1	16.21	5.31	28.66	1.05	0.00	0.19	12.57	13.82	0.00	14.68	0.00		92.49
98c6 4 2	16.48	5.51	29.26	1.30	0.00	0.00	12.60	12.64	0.05	15.43	0.04		93.31
98c1 3 1	6.27	3.82	39.41	1.15	0.00	0.00	14.79	6.79	7.04	16.62	0.14		96.03
98c1 3 2	5.70	3.05	40.28	0.78	0.00	0.15	16.27	9.27	1.00	15.70	0.14		92.34
PGE oxides													
98c3 2 2	14.75	6.25	44.44	1.33	0.00	0.00	10.73	0.89	0.04	0.12	0.01	22.78	101.34
98c3 2 3	14.59	6.65	43.12	0.95	0.00	0.13	10.00	1.21	0.00	0.13	0.00	22.08	98.86
98c3 1 1	16.71	7.78	36.26	1.58	0.00	0.00	11.02	0.91	0.04	0.15	0.04	20.92	95.41
98c3 1 2	16.97	7.69	35.68	0.86	0.00	0.53	10.82	0.67	0.00	0.11	0.00	20.60	93.93
98c3 1 3	16.66	9.48	36.37	0.97	0.00	0.35	8.85	1.10	0.00	0.09	0.00	20.34	94.21
98c7 1 1	21.00	7.51	37.64	1.09	0.00	0.00	9.72	0.95	0.00	0.09	0.00	21.41	99.41
98c7 1 2	17.41	6.57	36.56	1.21	0.00	0.00	12.34	0.78	0.09	0.06	0.09	21.39	96.50
98c7 1 3	18.17	7.19	34.69	1.20	0.00	0.00	13.78	0.83	0.00	0.08	0.06	21.65	97.65
98c6 1 2	16.93	9.14	39.21	2.47	0.00	0.00	11.82	1.84	0.00	0.11	0.00	23.09	104.61
98c6 1 3	17.13	10.24	38.80	1.35	0.00	0.43	11.63	1.08	0.06	0.07	0.05	22.64	103.48
98c1 4 1	13.27	6.04	32.41	0.48	0.00	0.02	20.38	1.11	0.14	0.02	0.22	22.51	96.60
98c1 4 2	11.41	5.40	33.45	1.07	0.00	0.00	19.55	1.14	0.09	0.02	0.15	22.33	94.61
98c2 2 1	14.60	10.16	41.34	1.44	0.00	0.00	11.37	1.25	0.00	0.05	0.06	22.84	103.11
PGE alloys													
98c2 1 1	0.95	4.45	0.00	1.44	46.73	0.00	17.25	25.20	1.04	0.10	0.35		97.51
98c1 2 2	0.35	5.21	0.02	0.89	47.18	0.00	17.18	23.04	1.08	0.09	0.10		95.14
0325i 3 9	0.52	3.65	0.00	2.36	43.46	0.93	21.95	21.16	1.19	0.12	0.26		95.60
0325i 3 10	0.41	18.61	0.11	2.12	29.53	0.13	24.51	20.76	1.33	0.09	0.24		97.84
98c1 2 1	0.16	28.38	0.00	0.77	29.91	0.00	25.01	13.27	0.52	0.11	0.16		98.29
98c1 2 2	0.13	19.73	0.00	0.96	34.51	0.00	21.17	20.84	0.35	0.08	0.28		98.05
0325i 3 7	22.51	29.69	18.93	2.43	2.97	0.00	13.84	6.54	0.38	0.05	0.00		97.34
0325i 3 8	17.99	23.75	14.09	2.36	11.11	0.00	16.28	9.83	0.79	0.12	0.00		96.32
0325i 3 5	20.03	25.72	14.42	2.34	10.41	0.10	15.82	9.68	0.55	0.09	0.00		99.16
0325f 3 1	25.60	20.20	37.87	3.43	0.00	0.00	9.36	1.70	0.13	0.00	0.51		98.80
Base-metal sulfides and alloys													
98c1 1 1	0.00	0.00	0.17	0.00	0.00	0.23	34.88	27.71	0.04	34.51	0.25		97.79
98c1 1 2	0.07	0.31	0.00	0.00	0.00	0.05	24.09	73.75	0.00	0.03	0.37		98.67
98c1 3	0.06	0.00	0.04	0.02	0.00	0.14	26.98	69.51	0.14	0.00	0.32		97.21

having crystallized in the upper few kilometers of the magmatic arc mantle (Bridges *et al.* 1995). Nevertheless, the Bragança chromitites show low TiO₂ content (<0.24 wt%). Chromite from ophiolites usually contains less than 0.3 wt% TiO₂ (*e.g.*, Leblanc & Nicolas 1992, Zhou & Bai 1992). The high TiO₂ content (~0.45 wt%) in chromite from podiform deposits is invariably associ-

ated systematically with Al-rich chromite, never with Cr-rich chromite as in the Loma Peguera chromitite (Zhou & Bai 1992, Melcher *et al.* 1997, Proenza *et al.* 1999).

In contrast, the chromite compositions in the Loma Peguera chromitites overlap with those of Uralian-Alaskan-type complexes (Figs. 10A, B). Bodies of

TABLE 4 (cont'd). SELECTED RESULTS OF ELECTRON-MICROPROBE ANALYSES OF PGM AND BASE-METAL MINERALS FROM THE LOMA PEGUERA CHROMITITE

	Os	Ir	Ru	Rh	Pt	Pd	Fe	Ni	Cu	S	As	O *
Laurite												
98c6 2 2 at.%	5.12	1.53	23.45	0.84	0.00	0.00	1.46	0.15	0.05	67.41	0.00	0.00
98c6 2 3	5.28	1.12	22.67	0.75	0.00	0.25	1.59	0.34	0.00	68.00	0.00	0.00
98c6 3 2	5.19	4.40	19.74	0.54	0.00	0.00	4.67	0.22	0.00	62.25	2.99	0.00
Unknown Ru₃As₂												
0325f 1 1	12.51	1.21	36.78	0.87	0.00	0.00	6.08	0.15	0.00	0.00	42.40	0.00
Partially desulfurized laurite												
98c6 4 1	6.42	2.08	21.37	0.77	0.00	0.14	16.97	17.74	0.00	34.52	0.00	0.00
98c6 4 2	6.46	2.14	21.59	0.94	0.00	0.00	16.82	16.05	0.05	35.89	0.04	0.00
98c1 3 1	2.25	1.36	26.61	0.76	0.00	0.00	18.07	7.89	7.56	35.37	0.13	0.00
98c1 3 2	2.13	1.13	28.27	0.53	0.00	0.10	20.66	11.20	1.11	34.73	0.13	0.00
PGE oxides												
98c3 2 2	3.53	1.48	20.00	0.59	0.00	0.00	8.74	0.69	0.03	0.17	0.01	64.76
98c3 2 3	3.60	1.62	20.01	0.43	0.00	0.06	8.40	0.97	0.00	0.18	0.00	64.73
98c3 1 1	4.33	2.00	17.69	0.76	0.00	0.00	9.73	0.76	0.03	0.23	0.03	64.45
98c3 1 2	4.48	2.01	17.72	0.42	0.00	0.25	9.73	0.60	0.00	0.17	0.00	64.65
98c3 1 3	4.47	2.52	18.35	0.48	0.00	0.17	8.08	0.95	0.00	0.14	0.00	64.84
98c7 1 1	5.35	1.89	18.05	0.51	0.00	0.00	8.43	0.78	0.00	0.14	0.00	64.85
98c7 1 2	4.41	1.65	17.44	0.57	0.00	0.00	10.65	0.64	0.07	0.09	0.06	64.43
98c7 1 3	4.54	1.78	16.31	0.56	0.00	0.00	11.73	0.67	0.00	0.11	0.04	64.28
98c6 1 2	3.98	2.12	17.33	1.07	0.00	0.00	9.46	1.40	0.00	0.15	0.00	64.48
98c6 1 3	4.11	2.43	17.53	0.60	0.00	0.19	9.51	0.84	0.04	0.10	0.03	64.62
98c1 4 1	3.14	1.41	14.42	0.21	0.00	0.01	16.41	0.85	0.10	0.03	0.13	63.29
98c1 4 2	2.73	1.28	15.05	0.47	0.00	0.00	15.92	0.88	0.07	0.02	0.09	63.49
98c2 2 1	3.48	2.39	18.53	0.63	0.00	0.00	9.23	0.96	0.00	0.07	0.04	64.68
PGE alloys												
98c2 1 1	0.48	2.22	0.00	1.34	22.95	0.00	29.58	41.12	1.57	0.30	0.44	0.00
98c1 2 2	0.18	2.71	0.02	0.86	24.16	0.00	30.74	39.21	1.69	0.28	0.14	0.00
0325i 3 9	0.26	1.80	0.00	2.18	21.10	0.83	37.24	34.14	1.77	0.35	0.33	0.00
0325i 3 10	0.20	8.86	0.10	1.89	13.85	0.11	40.17	32.62	1.92	0.25	0.30	0.00
98c1 2 1	0.08	14.91	0.00	0.75	15.38	0.00	44.92	22.68	0.82	0.35	0.21	0.00
98c1 2 2	0.06	9.92	0.00	0.90	17.09	0.00	36.62	34.28	0.53	0.25	0.36	0.00
0325i 3 7	13.67	17.85	21.63	2.73	1.76	0.00	28.63	12.87	0.70	0.18	0.00	0.00
0325i 3 8	10.37	13.55	15.28	2.51	6.24	0.00	31.95	18.35	1.36	0.40	0.00	0.00
0325i 3 5	11.47	14.57	15.53	2.48	5.81	0.11	30.85	17.95	0.94	0.30	0.00	0.00
0325f 3 1	15.77	12.32	43.92	3.90	0.00	0.00	19.65	3.39	0.25	0.00	0.79	0.00
Base-metal sulfides and alloys												
98c1 1 1	0.00	0.00	0.08	0.00	0.00	0.01	28.64	21.64	0.03	49.36	0.15	0.00
98c1 1 2	0.02	0.09	0.00	0.00	0.00	0.03	25.44	74.07	0.00	0.05	0.29	0.00
98c1 3	0.02	0.00	0.02	0.01	0.00	0.08	28.83	70.65	0.13	0.00	0.26	0.00

O*: calculated assuming a 4+ valence for PGE, 3+ valence for Fe, and 2+ valence for Ni and Cu (Garuti *et al.* 1997b).

chromitite of the Uralian–Alaskan type are small in size, and consist of centimetric segregations, schlieren, and lenses up to some meters in size (Garuti *et al.*

2003, 2005). However, the Uralian–Alaskan type represents concentrations of chromite in high-level (crustal section) concentrically zoned intrusions within the

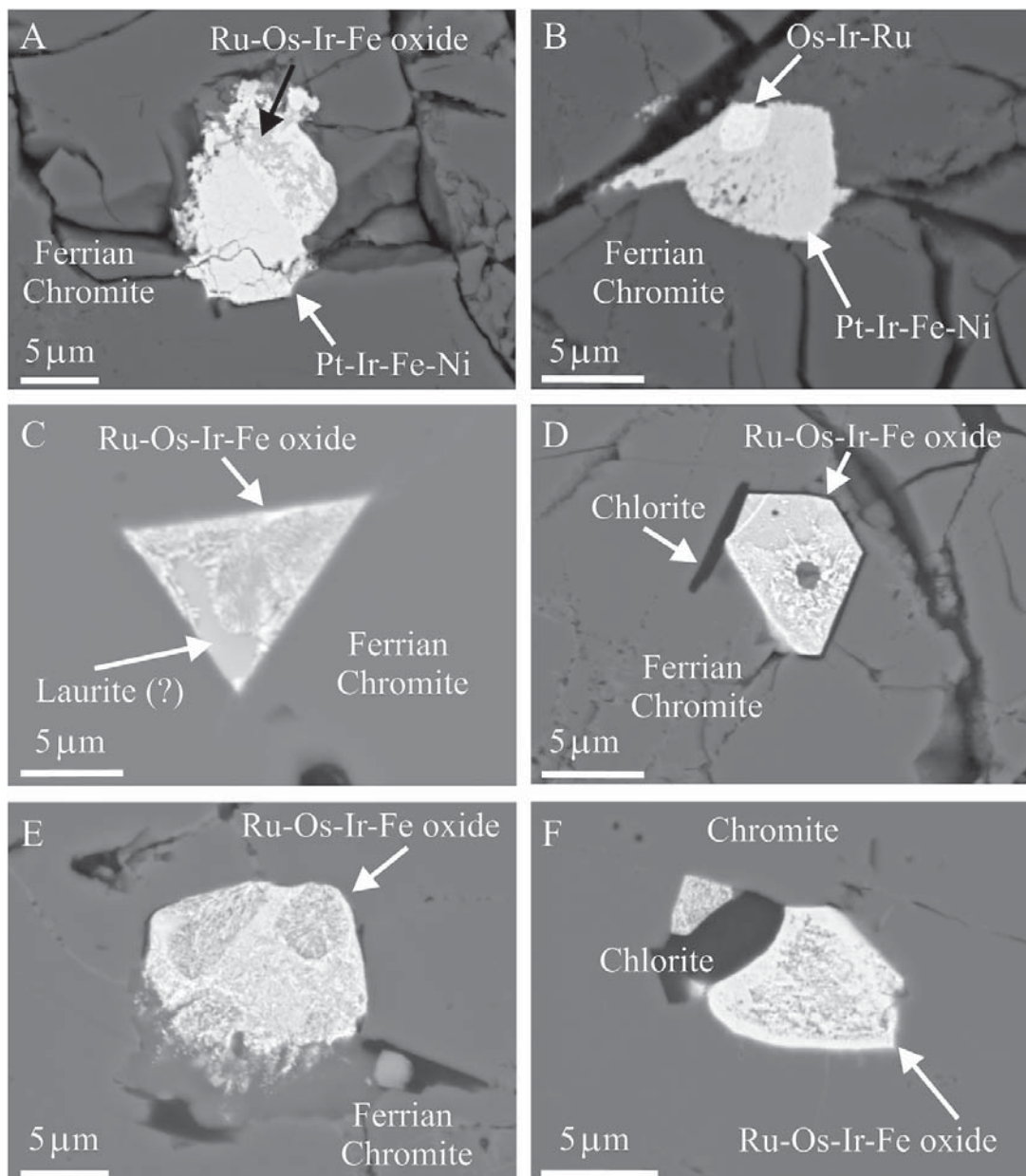
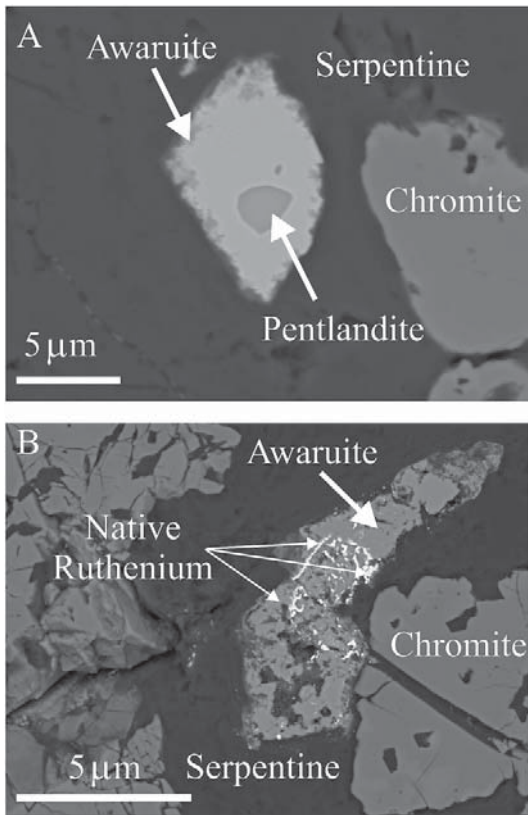


FIG. 6. BSE images showing morphology, texture and mineral assemblages of altered PGM in the Loma Peguera chromitites.

magmatic arc (Nixon *et al.* 1990, Garuti *et al.* 1997a), whereas the Loma Peguera chromitites are hosted in typical mantle peridotites.

Kamenetsky *et al.* (2001) confirmed that abundances of Al_2O_3 and TiO_2 in magmatic spinel are mainly controlled by concentrations of these oxides in the parental melts, and suggested the use of an Al_2O_3

versus TiO_2 diagram to discriminate among different magma-types, their tectonic setting and mantle sources. Chromite samples from Loma Peguera chromitites have Al_2O_3 and TiO_2 contents similar to those from Alaska-type complexes and island-arc series (Fig. 10C). Specifically they have compositions similar to spinel in picritic arc lavas from Vanuatu (Eggins 1993). We



calculated the Al_2O_3 and TiO_2 contents of the parental melts in equilibrium with the Loma Peguera chromitites using $(Al_2O_3)_{spinel}$ versus $(Al_2O_3)_{melt}$ and $(TiO_2)_{spinel}$ versus $(TiO_2)_{melt}$ systematic relationship in low-Al spinels (Kamenetsky *et al.* 2001). The results indicate that the melt had low Al contents (~ 10 wt% Al_2O_3) and relatively high Ti contents (0.7–1.1 wt% TiO_2). These values suggest derivation from high-Mg melts or an evolution toward higher-Ti tholeiitic or calc-alkaline compositions (*e.g.*, Tesalina *et al.* 2003), compared to the Cr-rich chromitites in an ophiolitic mantle, formed from Ti-depleted boninites (Zhou & Robinson 1997, Melcher *et al.* 1997, Proenza *et al.* 1999).

In addition, the composition of chromite from the Loma Peguera chromitites is close to that reported for chromian spinel from some oceanic plateau basalts (Fig. 10C). For example, spinel from Hole 462A (Nauru Basin Oceanic Plateau, southwestern Pacific) is characterized by a Cr# range from 0.54 to 0.73, TiO_2 from 0.5 to 0.8 wt%, and Fe_2O_3 from 6 to 9 wt% (Tokuyama & Batiza 1981). Spinel compositions from the Nauru Plateau basalts were not included in the compilation of basalt from Large Igneous Provinces (LIP) by Kamenetsky *et al.* (2001), as they plot in a separate field in Figure 10C.

FIG. 7. BSE images showing (A) pentlandite rimmed by awaruite, (B) awaruite containing small spots of native Ru.

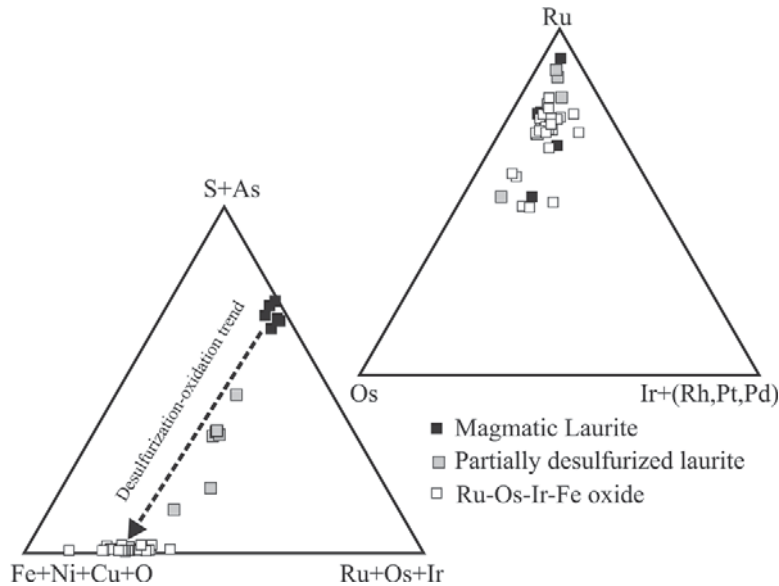


FIG. 8. Composition (atom %) of laurite and Ru–Os–Ir–Fe oxides in terms of $(S + As) - (Fe + Ni + Cu) - (Ir + Rh + Pt + Pd)$.

The genesis of Loma Peguera chromitite is still a matter of debate, and the results of this study do not lead to a conclusive answer. As pointed out above, and summarized in Figure 10, the Loma Peguera chromitites are different in spinel composition from ordinary ophiolitic chromitite, but they are hosted by ophiolitic mantle tectonite. The mechanism of chromite crystallization to form large volumes of chromitite in ophiolitic mantle rocks is controversial (*e.g.*, Paktunc 1990, Zhou & Robinson 1997). However, the most recent interpretations as to the genesis of Cr-rich chromitite in ophiolitic complexes point to a suprasubduction zone setting for the formation of podiform chromitites; they form by peridotite – melt reaction within conduits in the upper mantle (Arai & Yurimoto 1995, Zhou & Robinson 1997, Melcher *et al.* 1997, Proenza *et al.* 1999). Thus, tentatively, we suggest two possibilities to explain the “exotic” composition of Loma Peguera chromitites:

1) They result from interaction between a heterogeneous oceanic mantle (Loma Caribe peridotite) and Cretaceous island-arc-derived melts. Chromian spinel in island-arc environments shows a significant variation in TiO₂ content (Kamenetsky *et al.* 2001). The relatively high TiO₂ content of Loma Peguera chromite was possibly due to the evolved character of the melt involved.

2) They are a product of crystallization during percolation of magmas, from the Duarte or other plume, through a deep portion of suboceanic mantle (Loma Caribe peridotite). This hypothesis is consistent with the fact that Duarte-Complex-like mafic dykes

cut the Loma Caribe peridotite (Escuder-Viruete *et al.* 2006). Geochemical data show that the Duarte Complex includes high-Ti picrites, low-Ti, high-Mg basalts, and primitive high-Mg basalts, interlayered in the lowermost levels. These rocks are high in Cr (1050–1375 ppm) and Ni (375–850 ppm). On the other hand, restites for oceanic plateau basalt are peridotite containing chromian spinel with Cr# around 0.8 (Arai 1994), similar to dunites associated with Loma Peguera chromitites (Fig. 3A). If this hypothesis is viable, the Loma Peguera chromitite represents the first example of chromitite formed in a suboceanic upper mantle affected by a mantle plume.

These tectonic scenarios are consistent with the proposed origin and tectonic evolution of the Median belt ophiolite in the Dominican Republic (Draper *et al.* 1996). According to these authors, the ophiolite may consist of either 1) a suprasubduction-zone body, stratigraphically underlying the Maimon Formation (island-arc tholeiite), or 2) an association of the Loma Caribe peridotite with the metabasalts of the E-MORB Duarte complex, which has compositions comparable with those found on an oceanic plateau, related to a mantle plume.

Significance of the Pt-rich PGM assemblage

The PGE pattern of the Loma Peguera chromitites, in general, is similar to that of the chromitites hosted in the mantle sequence of the ophiolites, showing an enrichment in Os + Ir + Ru relative to Rh + Pd + Pt, which causes a negative slope between the IPGE and the PPGE. However, the total PGE concentrations are relatively high (up to more than 2 ppm) compared to the values generally reported for ophiolitic chromitites (generally less than 0.3 ppm). Furthermore, the Loma Peguera chromitites display a Pt anomaly with respect to Rh and Pd. Consistent with the high PGE concentration, the PGM are rather abundant in the Loma Peguera chromitites, and they comprise specific phases of Os–Ir–Ru, as typical for ophiolitic chromitites, accompanied by abundant Pt-bearing alloys, a feature of Alaskan-type chromitites (Garuti *et al.* 2003). The anomalous behavior of Pt is due to the stabilization of Pt-bearing alloys, whereas specific minerals of Rh and Pd were not found.

Platinum-bearing alloys, as found at Loma Peguera, are uncommon in ophiolitic chromitites elsewhere. Platinum–Fe–Ni alloys have been described by Corrivaux & Laflamme (1990) in PGE-rich chromitites from the Thetford Mines ophiolite complex, by Pedersen *et al.* (1993) in PGE-enriched chromitites within the mantle tectonite from the Leka ophiolite complex, and by Malitch *et al.* (2003) in banded chromitites from the Kraubath ophiolitic massif in Austria. Also, Prichard *et al.* (1994) reported undetermined Pt-bearing alloys from serpentinized and weathered chromite-rich rocks from Shetland, Scotland. Recently, they have been recorded

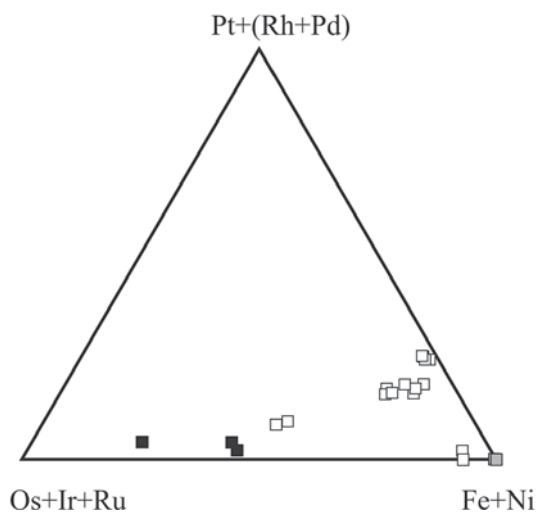


FIG. 9. Composition (atom %) of alloys containing base metals and the PGE in terms of (Pt + Rh + Pd) – (Os + Ir + Ru) – (Fe + Ni). Black squares: PGM alloys, open squares: PGE-bearing base-metal alloys, grey squares: PGE-free awaruite.

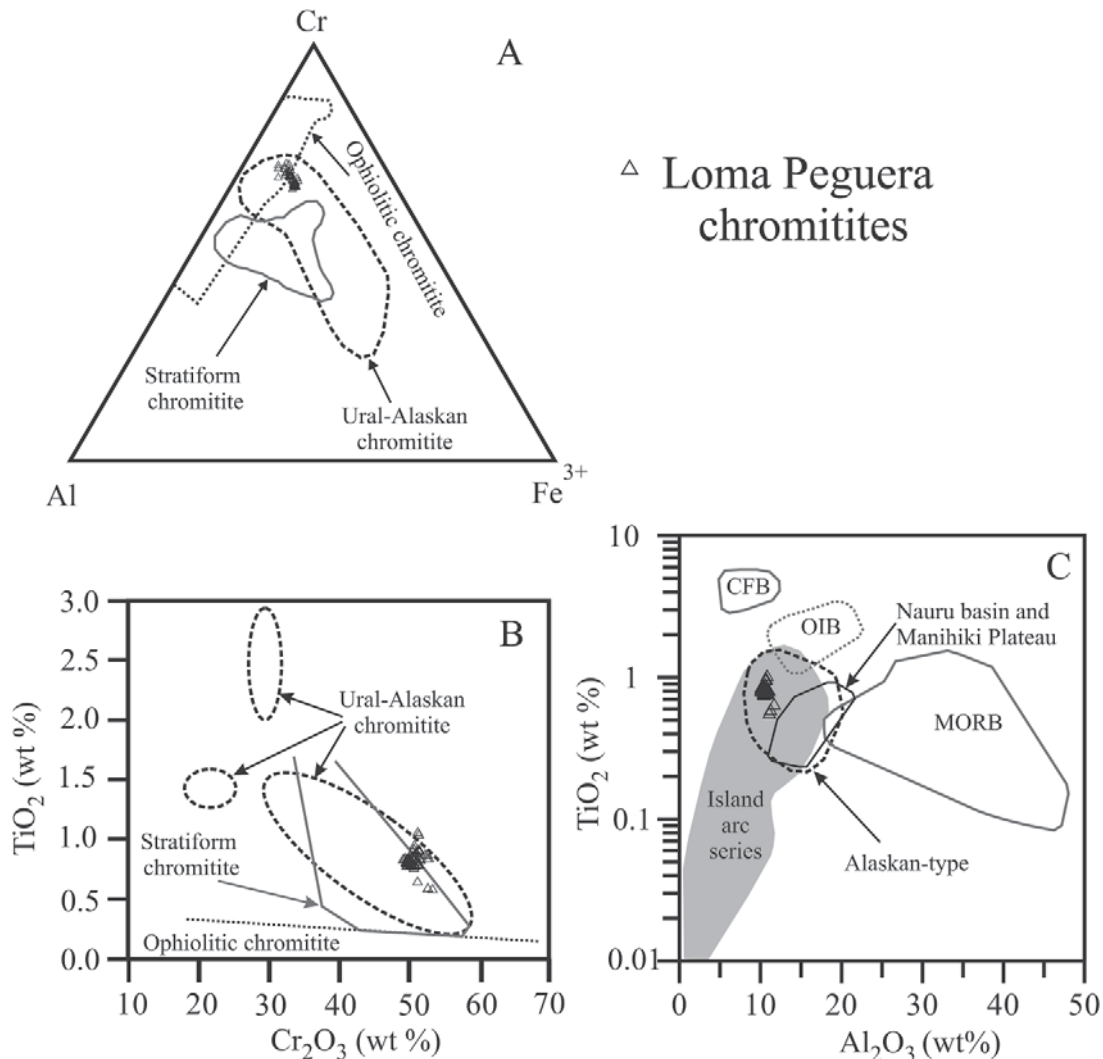


FIG. 10. Chemical composition of chromite from the Loma Peguera chromitite compared with that from the stratiform, ophiolitic and Ural-Alaskan chromitites of Urals. A) Cr–Al–Fe³⁺ atomic ratios. B) TiO₂ wt% versus Cr₂O₃ wt%. Note that the Loma Peguera chromitite plots within the field of the Ural-Alaskan chromitite. The boundaries between stratiform and podiform chromitites are from Arai *et al.* (2004) and Ferrario & Garuti (1987). Field of chromitite composition from Ural-Alaskan chromitites according to Garuti *et al.* (2005). C) Comparison of TiO₂ (wt%) and Al₂O₃ (wt%) contents in chromite from Loma Peguera with compositions of chromian spinel in volcanic and plutonic complexes from various geotectonic settings: Nauru basin and Manihiki oceanic plateaus after Tokuyama & Batiza (1981), Shcheka (1981) and Clague (1976). Data on Alaskan-type complexes are from the compilation of Batanova *et al.* (2005). Data on continental flood basalt (CFB), ocean island basalts (OIB), mid-ocean-ridge basalts (MORB), and island-arc series are from Kamenetsky *et al.* (2001).

from other PGE-rich chromitites such as in the Nurali complex, southern Urals (Zaccarini *et al.* 2004). Nevertheless, the Pt–Fe–Ni alloys described by these authors are Ir-poor and have higher Cu and Pd contents than those of the Loma Peguera chromitites.

Textural evidence and paragenetic assemblages indicate that the Pt-bearing alloys found in the Loma Peguera chromitites formed at a late stage after fracturing of chromite, probably associated with oxidation of chromite and the formation of chlorite. Usually, secondary PGM alloys are interpreted as resulting from

the removal of sulfur during serpentinization (Stockman & Hlava 1984, Garuti & Zaccarini 1997). However, all our analyzed Pt-bearing alloy grains are sulfur-free, suggesting complete desulfuration or the possibility that they were not generated by a desulfuration process. On the other hand, we note that PGM-bearing assemblages are Sb- and Te-free, elements usually interpreted to be introduced during the alteration of the primary minerals (Prichard *et al.* 1994). Thus, we do not believe that Pt was added to the chromitite from an external source during hydrothermal alteration. We suggest that the Pt-bearing alloys from Loma Peguera may represent the product of alteration of pre-existing Pt–Fe–Ni alloys, originally included in the chromite grains. They probably formed by reaction with hydrothermal fluids responsible for the oxidation of chromite and the formation of chlorite, and involving both *in situ* alteration of primary PGM and directed deposition from hydrothermal solutions.

Although it is difficult to determine the extent of PGE mobilization on the basis of mineralogical observations, the data presented here suggest that the alteration processes that affected the primary PGM in the Loma Peguera chromitites induced the redistribution of PGE on a small scale only. As a consequence, these secondary processes modified the primary PGM assemblage without changing the whole-rock concentration of the PGE.

ACKNOWLEDGEMENTS

We are indebted to our colleague Edwin Devaux, formerly at Falcondo, Bonaio, and Alex Butler, mine manager at Falcondo, for their continued support in our research on the Loma Caribe peridotite and laterites. F.Z. is grateful to the Austrian Science Fund (FWF Lise Meitner fellowship) for support for two years at the University of Leoben. Prof. J. Jedwab is thanked for the free electronic access to the useful "A bibliographic guide to unconventional Platinum Group Mineral and Mineraloids – UPGMM". The authors are also very grateful to Shoji Arai, Dogan Paktunc and an anonymous referee for their critical comments, as well as Bob Martin for his usual careful editing of the manuscript. We also acknowledge fruitful discussions with A. Pérez-Estaún (I.C.T. Jaime Almera – CSIC, Barcelona). This research has been in part financed by the Spanish research project CGL2004–00622.

REFERENCES

- ARAI, S. (1992): Chemistry of chromian spinel in volcanic rocks as a potential guide to magma chemistry. *Mineral. Mag.* **56**, 173-178.
- ARAI, S. (1994): Compositional variation of olivine – chromian spinel in Mg-rich magmas as a guide to their residual spinel peridotites. *J. Volcanol. Geotherm. Res.* **59**, 279-293.
- ARAI, S., UESUGI, J. & AHMED, A.H. (2004): Upper crustal podiform chromitite from the northern Oman ophiolite as the stratigraphically shallowest chromitite in ophiolite and its implication for Cr concentration. *Contrib. Mineral. Petrol.* **147**, 145-154.
- ARAI, S. & YURIMOTO, H. (1995): Possible sub-arc origin of podiform chromitites. *Island Arc* **4**, 104-111.
- BARNES, S.J. & ROEDER, P.L. (2001): The range of spinel compositions in terrestrial mafic and ultramafic rocks. *J. Petrol.* **42**, 2279-2302.
- BATANOVA, V.G., PERTSEV, A.N., KAMENETSKY, V.S., ARISKIN, A.A., MOCHALOV, A.G. & SOBOLEV, A.V. (2005): Crustal evolution of island-arc ultramafic magma: Galmoenan pyroxenite–dunite plutonic complex, Koryak Highland (Far East Russia). *J. Petrol.* **46**, 1345-1366.
- BOWIN, C.O. (1966): Geology of the central Dominican Republic (a case history of part of an island arc). In Caribbean Geological Studies (H. Hess, ed.). *Geol. Soc. Am., Mem.* **98**, 11-84.
- BRIDGES, J.C., PRICHARD, H.M. & MEIRELES, C.A. (1995): Podiform chromitite-bearing ultramafic rocks from the Bragança Massif, northern Portugal: fragments of island arc mantle? *Geol. Mag.* **132**, 39-49.
- CAWTHORN, R.G. (1999): The platinum and palladium resource of the Bushveld complex. *S. Afr. J. Sci.* **95**, 481-489.
- CLAGUE, D.A. (1976): Petrology of basaltic and gabbroic rocks dredged from Danger Island Troughs, Manihiki Plateau. *Init. Rep. D.S.D.P.* **33**, 891-911.
- CORRIVAUX, L. & LAFLAMME, J.H.G. (1990): Minéralogie des éléments du groupe du platine dans les chromitites de l'ophiolite de Thetford Mines, Québec. *Can. Mineral.* **28**, 579-595.
- DRAPER, G., GUTIÉRREZ, G. & LEWIS, J.F. (1996): Thrust emplacement of the Hispaniola peridotite belt: orogenic expression of the mid-Cretaceous Caribbean arc polarity reversal? *Geology* **24**, 1143-1146.
- ECONOMOU ELIOPOULOS, M. (1996): Platinum-group elements distribution in chromite ores from ophiolite complexes: implications for their exploration. *Ore Geol. Rev.* **11**, 363-381.
- EGGINS, S.M. (1993): Origin and differentiation of picritic arc magmas, Ambae (Aoba), Vanuatu. *Contrib. Mineral. Petrol.* **114**, 79-100.
- ESCUDEYR-VIRUETE, J., HERNANDEZ HUERTA, P.P., DRAPER, G., GUTIÉRREZ, G., LEWIS, J.F. & PÉREZ-ESTAÚN, A. (2002): Metamorfismo y estructura de la Formación Maimón y los complejos Duarte y Río Verde, Cordillera Central Dominicana: implicaciones en la estructura y la evolución del primitivo arco isla caribeño. *Acta Geologica Hispanica* **37**, 123-162.

- ESCUDER-VIRUETE, J., PÉREZ-ESTAÚN, A., CONTRERA, F., JOUBERT, M., WEIS, D., ULLRICH, T.D. & SPADEA, P. (2006): Plume mantle source heterogeneity through time: insights from the Duarte Complex, Hispaniola, north-eastern Caribbean. *J. Geophys. Res.* **112**, B04203, doi: 10.1029/2006JB004323.
- FERRARIO, A. & GARUTI, G. (1987): Platinum-group minerals in chromite-rich horizons of the Niquelandia complex (central Goiás, Brazil). *In* Geo-Platinum 87 (H.M. Prichard, P.J. Potts, J.F.W. Bowles & S. Cribb, eds.). Elsevier Applied Science, London, U.K. (261-272).
- GARUTI, G., FERSHTATER, G., BEA, F., MONTERO, P., PUSHKAREV, E.V. & ZACCARINI, F. (1997a): Platinum-group elements as petrological indicators in mafic-ultramafic complexes of the central and southern Urals: preliminary results. *Tectonophysics* **276**, 181-194.
- GARUTI, G., PUSHKAREV, E.V. & ZACCARINI, F. (2005): Diversity of chromite-PGE mineralization in ultramafic complexes of the Urals. *In* Platinum-Group Elements – from Genesis to Beneficiation and Environmental Impact (T.O. Törmänen & T.T. Alapieti, eds.). *Tenth Int. Platinum Symp. (Oulu)*, 341-344.
- GARUTI, G., PUSHKAREV, E.V., ZACCARINI, F., CABELLA, R. & ANIKINA, E.V. (2003): Chromite composition and platinum-group mineral assemblage in the Uktus Alaskan-type complex (central Urals, Russia). *Mineral. Deposita* **38**, 312-326.
- GARUTI, G. & ZACCARINI, F. (1997): *In situ* alteration of platinum-group minerals at low temperature: evidence from serpentinized and weathered chromitite of the Vourinos complex, Greece. *Can. Mineral.* **35**, 611-626.
- GARUTI, G., ZACCARINI, F., CABELLA, R. & FERSHTATER, G. (1997b): Occurrence of unknown Ru–Os–Ir–Fe oxides in the chromitites of the Nurali ultramafic complex, southern Urals, Russia. *Can. Mineral.* **35**, 1431-1439.
- GARUTI, G., ZACCARINI, F. & ECONOMOU-ELIPOPOULOS M. (1999a): Paragenesis and composition of laurite in chromitites of Othrys (Greece): implication for Os–Ru fractionation in ophiolitic upper mantle of the Balkan Peninsula. *Mineral. Deposita* **34**, 312-319.
- GARUTI, G., ZACCARINI, F., MOLOSHAG, V. & ALIMOV, V. (1999b): Platinum-group minerals as indicators of sulfur fugacity in ophiolitic upper mantle: an example from chromitites of the Ray–Iz ultramafic complex, Polar Urals, Russia. *Can. Mineral.* **37**, 1099-1115.
- GAUTHIER, M., CORRIVAUX, L., TROTTIER, L.J., CABRI, L.J., LAFLAMME, J.H.G. & BERGERON, M. (1990): Chromitites platinifères de l'Estrie-Beauce, Appalaches du sud de Québec. *Mineral. Deposita* **25**, 169-178.
- GERVILLA, F., PROENZA, J.A., FREI, R., GONZÁLEZ-JIMÉNEZ, J.M., GARRIDO, C.J., MELGAREJO, J.C., MEIBOM, A., DÍAZ-MARTÍNEZ, R. & LAVAUT, W. (2005): Distribution of platinum-group elements and Os isotopes in chromite ores from Mayarí–Baracoa ophiolitic belt (eastern Cuba). *Contrib. Mineral. Petrol.* **150**, 589-607.
- HALDEMANN, E.G., BUCHAN, R., BLOWES, V.H. & CHANDLER, T. (1979): Geology of the laterite nickel deposits, Dominican Republic. *In* International Laterite Symposium (D.J. Evans, R.S. Shoemaker & H. Velman, eds.). Society of Mining Engineers, New Orleans, Louisiana (57-84).
- IRVINE, T.N. (1967): Chromian spinel as a petrogenetic indicator. II. Petrologic applications. *Can. J. Earth Sci.* **4**, 71-103.
- KAMENETSKY, V.S., CRAWFORD, A.J. & MEFFRE, S. (2001): Factors controlling chemistry of magmatic spinel: an empirical study of associated olivine, Cr-spinel and melt inclusions from primitive rocks. *J. Petrol.* **42**, 655-671.
- KOJONEN, K., ZACCARINI, F. & GARUTI, G. (2003): Platinum-group elements and gold geochemistry and mineralogy in the Ray–Iz ophiolitic chromitites, Polar Urals. *In* Mineral Exploration and Sustainable Development (D.G. Eliopoulos *et al.*, eds.). Millpress, Rotterdam, The Netherlands (599-602).
- LEBLANC, M. & NICOLAS, A. (1992): Les chromitites ophiolitiques. *Chronique de la Recherche Minière* **507**, 3-25.
- LEWIS, J.F., ASTACIO, V.A., ESPAILLAT, J. & JIMENEZ, J. (2000): The occurrence of volcanogenic massive sulphide deposits in the Maimón Formation, Dominican Republic: the Cerro de Maimón, Loma Pesada and Loma Barbuito deposits. *In* VMS Deposits of Latin America (R. Sherlock & M.A.V. Logan, eds.). *Geol. Soc. Can., Spec. Publ.* **2**, 223-249.
- LEWIS, J.F. & DRAPER, G. (1990): Geological and tectonic evolution of the northern Caribbean margin. *In* Decade of North American Geology. H. The Caribbean. Geological Society of America, Boulder, Colorado (77-140).
- LEWIS, J.F., DRAPER, G., PROENZA, J.A., ESPAILLAT, J. & JIMENEZ, J. (2006): Ophiolite-related ultramafic rocks (serpentinites) in the Caribbean region: a review of their occurrence, composition, origin, emplacement and Ni-laterite soils. *Geologica Acta* **4**, 237-263.
- LEWIS, J.F., ESCUDER-VIRUETE, J., HERNAIZ-HUERTA, P.P., GUTIÉRREZ, G., DRAPER, G. & PÉREZ-ESTAÚN, A. (2002): Subdivisión geoquímica del arco de Isla Circum-Caribeño, Cordillera Central Dominicana: implicaciones para la formación, acreción y crecimiento cortical en un ambiente intraoceánico. *Acta Geol. Hisp.* **37**, 81-122.
- LEWIS, J.F. & JIMENEZ, G.J.G. (1991): Duarte Complex in the La Vega – Jarabacoa – Janico area, central Hispaniola; geological and geochemical features of the sea floor during early stages of arc evolution. *In* Geologic and Tectonic Development of North America – Caribbean plate boundary in Hispaniola (P. Mann, G. Draper & J.F. Lewis, eds.). *Geol. Soc. Am., Spec. Pap.* **262**, 115-141.
- LEWIS, J.F., PROENZA, J.A. & LONGO, F. (2005): New petrological and geochemical constraints on the origin of Loma

- Caribe peridotite (Dominican Republic). *Seventeenth Caribbean Geol. Conf. (Puerto Rico), Abstr. Vol.*, 47-48.
- LORAND, J.P. & CEULENEER, G. (1989): Silicate and base-metal sulfide inclusions in chromites from the Maqsad area (Oman ophiolite, Gulf of Oman): a model for entrapment. *Lithos* **22**, 173-190.
- MALITCH, K.N., JUNK, S.A., THALHAMMER, O.A.R., MELCHER, F., KNAUF, V.V., PERNICKA, E. & STUMPFL, E.F. (2003): Laurite and ruarsite from podiform chromitites at Kraubath and Hochgrößen, Austria: new insights from osmium isotopes. *Can. Mineral.* **41**, 331-352.
- MARCHESI, C., GARRIDO, C.J., GODARD, M., PROENZA, J.A., GERVILLA, F. & BLANCO-MORENO, J. (2006): Petrogenesis of highly depleted peridotites and gabbroic rocks from Mayarí-Baracoa ophiolitic belt (eastern Cuba). *Contrib. Mineral. Petrol.* **151**, 717-736.
- McELDUFF, B. & STUMPFL, E.F. (1990): The chromite deposits of the Troodos complex, Cyprus – evidence for the role of a fluid phase accompanying chromite formation. *Mineral. Deposita* **26**, 307-318.
- MELCHER, F., GRUM, W., SIMON, G., THALHAMMER, V.T. & STUMPFL, E.F. (1997): Petrogenesis of the ophiolitic giant chromite deposits of Kempirsai, Kazakhstan: a study of solid and fluid inclusions in chromite. *J. Petrol.* **38**, 1419-1458.
- NALDRETT, A. & DUKE, J.M. (1980): Pt metals in magmatic sulfide ores. *Science* **208**, 1417-1424.
- NICOLAS, A. (1989): *Structures of Ophiolites and Dynamics of Oceanic Lithosphere*. Kluwer Academic Publisher, Dordrecht, The Netherlands.
- NIXON, G.T., CABRI, L.J. & LAFLAMME, J.H.G. (1990): Platinum-group-element mineralization in lode and placer deposits associated with the Tulameen Alaskan-type complex, British Columbia. *Can. Mineral.* **28**, 503-535.
- PAKTUNC, A.D. (1990): Origin of podiform chromite deposits by multistage melting, melt segregation and magma mixing in the upper mantle. *Ore Geol. Rev.* **5**, 211-222.
- PARKINSON, I.J. & PEARCE, J.A. (1998): Peridotites from the Izu – Bonin – Mariana forearc (ODP Leg 125): evidence for mantle melting and melt–mantle interaction in a supra-subduction zone setting. *J. Petrol.* **39**, 1577-1618.
- PEDERSEN, R-B., JOHANNESSEN, G.M. & BOYD, R. (1993): Stratiform platinum-group element mineralization in the ultramafic cumulates of the Leka ophiolite complex, central Norway. *Econ. Geol.* **88**, 782-803.
- PRICHARD, H.M., IXER, R.A., LORD, R.A., MAYNARD, J. & WILLIAMS, N. (1994): Assemblages of platinum-group minerals and sulfides in silicate lithologies and chromite-rich rocks within the Shetland ophiolite. *Can. Mineral.* **32**, 271-294.
- PROENZA, J., GERVILLA, F., MELGAREJO, J.C. & BODINIER, J.-L. (1999): Al- and Cr- rich chromitites from the Mayarí-Baracoa ophiolitic belt (eastern Cuba): consequence of interaction between volatile-rich melts and peridotites in suprasubduction mantle. *Econ. Geol.* **94**, 547-566.
- PROENZA, J., ORTEGA-GUTIÉRREZ, F., CAMPRUBÍ, A., TRITLLA, J., ELÍAS-HERRERA, M. & REYES-SALAS, M. (2004): Paleozoic serpentinite-enclosed chromitites from Tehuiztzingo, (Acatlan complex, southern Mexico): a petrological and mineralogical study. *J. S. Am. Earth Sci.* **16**, 649-666.
- SHCHEKA, S. (1981): Igneous rocks of Deep Sea Drilling Project Leg 61, Nauru Basin. *Init. Rep. D.S.D.P.* **61**, 633-646.
- STOCKMAN, H.W. & HLAVA, P.F. (1984): Platinum-group minerals in alpine chromitites from southwestern Oregon. *Econ. Geol.* **79**, 491-508.
- TESALINA, S.G., NIMIS, P., AUGÉ, T. & ZAYKOV, V.V. (2003): Origin of chromite in mafic–ultramafic-hosted hydrothermal massive sulfides from the Main Uralian Fault, South Urals, Russia. *Lithos* **70**, 39-59.
- THAYER, T.P. (1964): Principal features and origin of podiform chromite deposits, and some observations in the Guleman–Soridağ district, Turkey. *Econ. Geol.* **59**, 1497-1524.
- TOKUYAMA, H. & BATIZA, R. (1981): Chemical composition of igneous rocks and origin of the sill and pillow-basalt complex of Nauru Basin, southwest Pacific. *Init. Rep. D.S.D.P.* **61**, 673-687.
- ZACCARINI, F., PROENZA, J.A., ORTEGA-GUTIERREZ, F. & GARUTI, G. (2005): Platinum group minerals in ophiolitic chromitites from Tehuiztzingo (Acatlán complex, southern Mexico): implications for metamorphic modification. *Mineral. Petrol.* **84**, 147-168.
- ZACCARINI, F., PUSHKAREV, E.V., FERSHTATER, G.B. & GARUTI, G. (2004): Composition and mineralogy of PGE-rich chromitites in the Nurali lherzolite–gabbro complex, southern Urals, Russia. *Can. Mineral.* **42**, 545-562.
- ZHOU, MEI-FU & BAI, WEN-JI (1992): Chromite deposits in China and their origin. *Mineral. Deposita* **27**, 192-199.
- ZHOU, MEI-FU & ROBINSON, P.T. (1997): Origin and tectonic environment of podiform chromite deposits. *Econ. Geol.* **92**, 259-262.
- ZHOU, MEI-FU, SUN, MIA, KEAYS, R.R. & KERRICH, R.W. (1998): Controls on platinum-group elemental distributions of podiform chromitites: a case study of high-Cr and high-Al chromitites from Chinese orogenic belts. *Geochim. Cosmochim. Acta* **62**, 677-688.

Received January 16, 2006, revised manuscript accepted April 11, 2007.